

STUDY OF ITB FORMATION AND SUSTAINMENT WITH OPTIMIZED CURRENT PROFILES IN THE HIGH-PERFORMANCE STEADY STATE PLASMA ON EAST

H.Q. Liu^{1*}, Y.Q.Chu¹, W. Z. Mao², H.Lian¹, S.X.Wang¹, S.B.Zhang¹, J.P. Qian¹, Y. Yang¹, L. Zeng¹, J. L. Xie², Y.X.Jie¹, X. Gao¹, X. Z. Gong¹, W.X. Ding², K. Hanada³, Y. F. Liang¹, N. Xiang¹, X.D. Zhang¹, B.N. Wan¹ and EAST Team

¹*Institute of Plasma Physics, Chinese Academy of Sciences, Hefei, 230031, China*

²*University of Science and Technology of China, Hefei, Anhui 230026, China*

³*Research Institute for Applied Mechanics, Kyushu University, Kasuga, Fukuoka, 816-8580, Japan*

Email: hqliu@ipp.ac.cn

ABSTRACT

Improve high-performance steady state plasma operation has been achieved on EAST with high β and optimized of current profile. Better confinement with e-ITB was obtained with flat central safety factor q profile in the core area, and the minimum q is slightly above unity contributing to sawteeth free plasma. Core magnetic fluctuation and reconstructed current profile dynamics are provided with the 11 chords polarimeter-interferometer measurement for those discharges, in which a low frequency long live helical mode structure is observed in the core area from the early time of these discharges and persists for a few times the current relaxation period. The characteristics of the internal mode evolution are analyzed spatially and temporally. It is inferred that the mode may be a saturated mode and plays an important role for sustained flat q profile operation by correlation analysis. The internal transport barrier (ITB) and edge transport barrier (ETB) are both observed with a optimized reverse shear q profile with MHDs like Alfvén cascades and reverse-sheared Alfvén eigenmode (RSAE). In the high-performance steady state plasma in EAST, the optimized current profiles and current induced fluctuations may play a role for ITB formation and sustainment. The ITBs with different current profiles and core fluctuations are presented.

1. INTRODUCTION

Recently, improved high-performance plasma operation has been significantly extended towards more ITER and CFETR related high beta steady-state regime with optimization of current profile ($\beta_P \sim 2.5$ & $\beta_N \sim 1.9$ with ITB + ETB of using RF & NB and $\beta_P \sim 1.9$ & $\beta_N \sim 1.5$ with eITB + ETB of using pure RF) on EAST [1-3]. The ITB formation and sustainment company with optimization of the current profiles, which seem to be due to different MHD-modes, similar with other devices [4-6]. The mechanisms of linking the observed changes in MHD-behaviour and current profile seem to play an important role for ITB formation and sustainment in high beta steady state plasma on EAST. A typical property of high β_N operation is formation of the internal transport barrier (ITB) in profiles of ion temperature, electron temperature and electron density separately or simultaneously[1]. In the high β_N experiments on EAST, the plasma is mainly heated by NBI and LHW and the β_N reaches to 1.9.

ITB has been widely studied in various tokamaks for years[4-11]. With reduced anomalous transport in core region, a high confinement performance could be achieved. In the past works, relations have been verified between ITB and factors like q profiles[12], MHD behaviors[13], Er profiles[14], etc. ITB can be formed by changing q profiles with unaltered E×B shearing rate[12], reducing turbulence growth rate plays a big role in better confinement. MHD behaviors are always mentioned with rational magnetic surface where ITB foot located and the effect of locally enhanced shear should be emphasized [13]. In terms of Er profile, it can be modified by plasma rotation velocity[14] and redistribution of energetic ions[15], finally, E×B shearing rate can be improved and low turbulence transport is achieved, then ITB could exist. The exploration of ITB triggering condition, essentially, is finding a state with anomalous transport reduced.

In this article, several discharges with ITB are discussed as typical shots in the high β experiments. In which, Different magnetic shear conditions provide opportunity to study the relations between ITB formation with q profiles. Several different types of MHD in the three discharges also verified the effect of MHD in ITB formation and sustainment. Besides, decoupling of q profiles and MHD behaviors give a chance to distinguish which one is predominating in ITB formation. Er shear shows predominance in most circumstances, while what should be

noted is the contribution of energetic particles redistributed by energetic particle modes[16,17], but not the portion come from plasma rotation. Under suitable conditions for ITB formation, power threshold should be considered then. Previous work on ITB about power threshold focus on the total heating power, however, it is the heating efficiency on ions and electrons that should pay more attention to according to the analysis of these ITB discharges..

2. EXPERIMENTAL SETUP

EAST is a tokamak aiming to long pulse stable high-performance plasma operation with major radius $R=1.85\text{m}$ and minor radius $a=0.45\text{m}$. Max toroidal magnetic field B_T is around 3.5T and plasma current I_p can be up to 1MA [18,19]. For the ITB experiments mentioned in this paper, EAST is operated with upper single null divertor configuration and the toroidal magnetic field is around 1.6T . Two main auxiliary heating systems are applied to heat the plasma, including LHW with frequency of 2.45GHz and 4.6GHz [20] and NBI with co-current direction and counter-current direction [21] that may influence plasma toroidal rotation velocity. In this article, control of NBI power is realized by adjusting quantities of NBI beams and power for each beam.

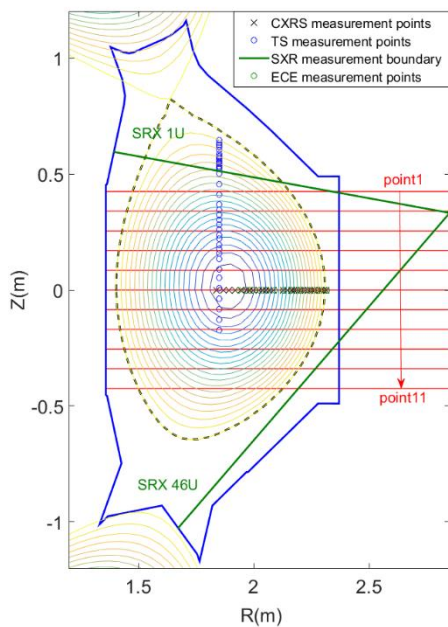


Fig. 1 Poloidal view of main diagnostics for data analysis

Main kinetic profiles analysis include plasma electron density n_e , ion temperature T_i , electron temperature T_e , and safety factor q profile. Charge exchange recombination spectroscopy(CXRS) is used to provide ion temperature and toroidal rotation profiles[22]. The tendency of T_i evolution can be obtained by the imaging x-ray crystal spectrometer(XCS)[23]. Electron temperature profile is from Thomson scattering(TS) system[24]. Due to the designed toroidal magnetic condition for electron cyclotron emission(ECE) is not suitable in these experiments, T_e profile from ECE is not available [25]. however, it still can be used to determine MHD position cooperating with soft X-ray (SXR) signals. Polarimeter-interferometer(POINT) system is utilized to measure the line integrated density and the faraday rotation angle [26], with spatial resolution of 0.085m and time resolution up to $1\ \mu\text{s}$, it is a powerful tool to measure key plasma parameters on EAST. Corresponding diagnostics system configurations are shown in figure 1, red line stands the POINT system measurement chords' position, By Abel-inversion method, the 11 measured line-integrated plasma density can provide density profile with high time resolution[27], additionally, taking density measurement in

core region from TS system and pedestal region from reflectometry system as reference, the fitted density profile can be more reliable. Using the faraday rotation as the additional constrained in EFIT code, q profile and current profile can be inferred[29].

Plasma parameters for the three high β_N discharges with ITB are shown in figure 2. Plasma current of #71326 and #80496 is 450kA , while for #71320 it is 400kA . They all have the same current ramping-up rate at about 280kA/s . Maximum β_N for three shots are close around 1.9 while the lasting period is determined by different conditions. Auxiliary heating systems for these shots are NBI and LHW. For #71320 and #71326, NBI is injected at 2.5s with 4 steps which corresponds to sources of 1L, 1R, 2L and 2R with interval of 0.5s . For #80496, NBI is injected at 3s with same sequence except the last 2R source. Power of each NBI beam is same in these shots, consequently, the NBI injecting power for #80496 is less than the other two shots. While in #80496, 2.45GHz LHW power with 0.5MW and 4.6GHz LHW whose power is set to increase from 0 to 2MW gradually and keep for few seconds are all applied.

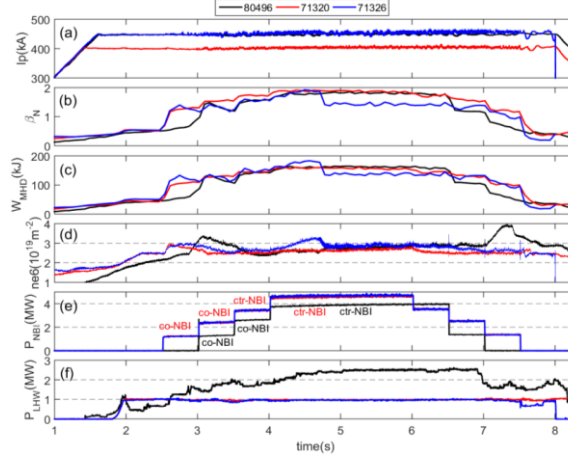


Fig.2 Three typical discharges, #80496(black line), #71320(red line), #71326(blue line). (a) Plasma current(I_p), (b) normalized beta(β_N), (c) stored energy, (d) core line-averaged density, (e) NBI power, (f) total power of 2.45GHz LHW and 4.6GHz LHW..

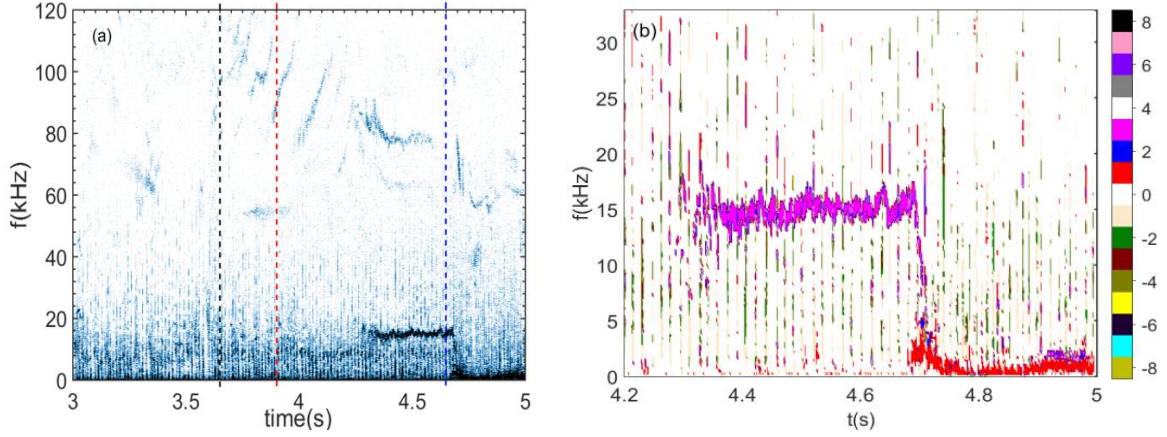


Fig.3 MHD observation in #71326. (a) spectrum of the 6th chord for density measurement of POINT, three vertical dash lines are time slices corresponding to 3.65s (black), 3.9s (red), 4.65s (blue), (b) enlargement of time window of 4.2-5s in(a), the toroidal phase spectrum over toroidal azimuth difference averaged toroidal mode number.

With different operational configurations, different MHD activities are observed and the corresponding safe factor (q) profiles are obtained from EFIT equilibrium reconstructed with POINT constraints in these three shots. The spectrum of the 6th channel density signal of POINT from 3s to 5s for #71326 is shown in figure 3. Around 3.6s, a grand cascade occur and last about 200ms, implying a process that q_{min} passes through rational surface [16,30-33], which should be 2 from the q profiles shown in figure 4. After that, reverse-sheared Alfvén eigenmode (RSAE) and beta-induced Alfvén eigenmode (BAE) dominate the high frequency region [30]. At 3.9s, q profile still presents as reversed, q_{min} keeps going down and the reversed region gets broaden. With the tendency continuing, q_{min} eventually stabilizes around 1.33 at the position of $\rho \sim 0.42$. As good precondition, a 4/3 kink mode appears at q_{min} position. Figure 3(b) shows the toroidal phase spectrum over toroidal azimuth difference averaged toroidal mode number. The spectrum is obtained from high frequency magnetic probes installed in toroidal direction. Due to the weak reversal shear configuration, difference q values near the q_{min} surface are small. Thus, this 4/3 kink mode could be observed in wide range near the q_{min} surface on ECE signal. However, the instinct 4/3 kink mode transits to a double tearing mode just after its appearance for about 300ms [34]. The relation between this kink mode and confinement will be discussed in next section.

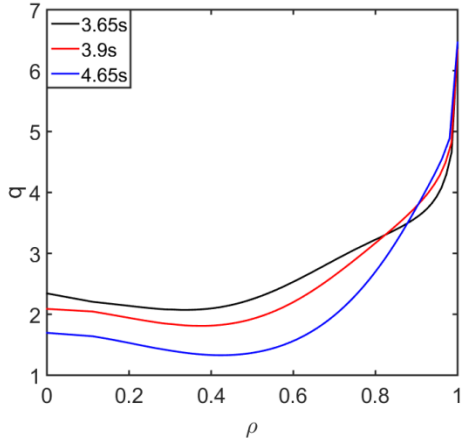


Fig.4 q profiles of #71326 at 3.65s (black line), 3.9s (red line) and 4.65s (blue line).

RSAE is also observed in the spectrum of POINT density signal for #80496 as shown in figure 5(a). What should be noted is the POINT density signal is contaminated by various electrical disturbance with fixed frequency along the discharge, but RSAE still can be identified in the spectrum. The reconstructed q profiles for 6 time slices from 3.7s to 5.4s show a reversal shear configuration (figure 8e). With the last ctr-NBI beam injecting at 4s and LHW power increasing, q profile evolves as central region flattening with q_0 around 1 gradually. Then q profiles keep similar until fishbone instability triggering at 4.78s as shown in figure 5(b). During the process, instead of the coupling between effect of $q \sim 1$ profile and fishbone, an interesting thing is the central q profiles keep flat and q_0 stay around 1 while MHD activities free, which provides a chance to decouple the two factors for understanding their predominating effects separately.

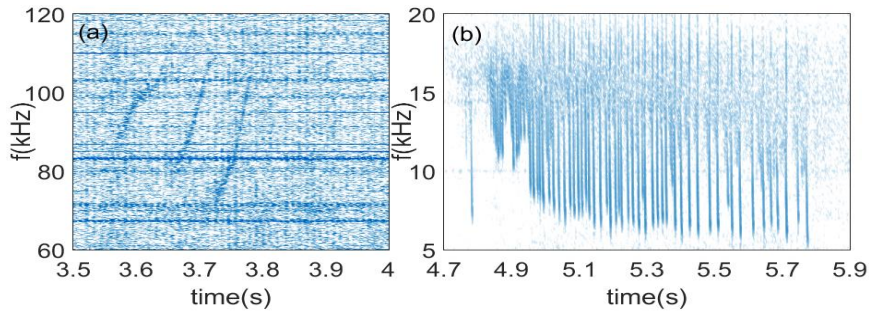


Fig.5 Spectrum of #80496 , (a) RSAE, (b) fishbone instability.

In terms of the last shot #71320, it is a good candidate for fishbone study. Figure 7 shows spectrum of SXR signal, time range is chosen to coverage three phases of fishbone with different characteristics. As shown in figure 7 , the amplitude and burst cycle of fishbone are varied with each NBI injecting step. Difference of frequency likely from rotation bulk plasma [35] indicates that energies of resonance energetic particles are similar. The amplitude of fishbone increases along with NBI injecting into plasma as proportion of energetic particles pressure is increasing. Shorter intervals between two adjoint fishbone manifests the state tends to be stable, and the corresponding q profile recovers to initial state quickly. Second harmonic generation shown in figure 6 illustrates a flat q profile which could be approved by the q profiles shown in figure 6. Highly similar q profiles in the inner region make the effect of fishbone be highlight. Details will be discussed in further work.

Positive magnetic shear is not optimized in EAST high β_N experiment because in present conditions q_0 is always less than 1 which lead to sawtooth instability. Sawtooth will expel particles and energy from plasma core that is on the contrary with the object of ITB formation. It is neither suitable for us to carry out ITB research nor a good candidate for high confinement experiment.

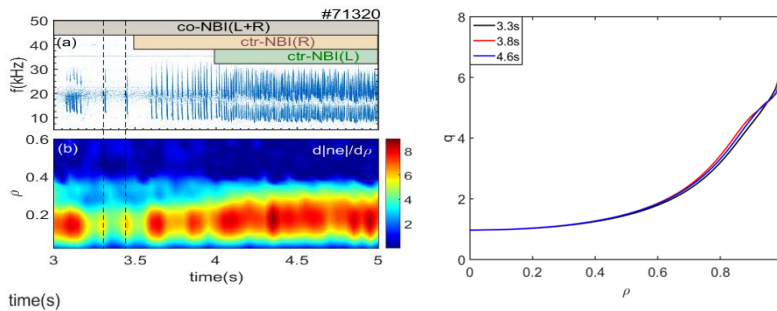


Fig.6 (left-a) Spectrum of SXR signal in #71320, square frames represent the duration of each NBI beam; (left-b) evolution of density gradient by POINT data; (right) q profiles of #71320.

3. EXPERIMENTAL RESULTS

The ITB and ETB are both observed with an optimized flat central q profile in the long-pulse high β_N

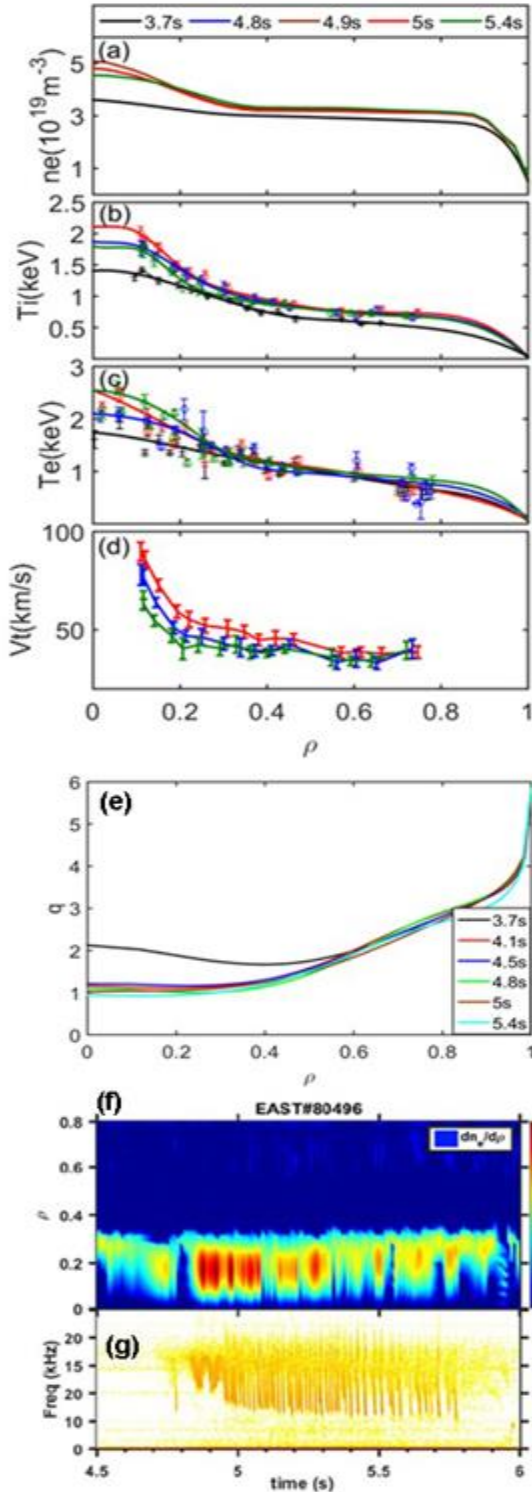


Fig.7. Kinetic profiles (a-d), q profiles (e) and the electron density gradient contour-plot (f) and the $m/n = 1/1$ fishbone (g) analysis with ITB discharge #80496.

operation, as shown in Figure 7. The ITB of ion temperature, electron temperature and electron density has been obtained simultaneously with the fishbone event. And the ITB+ETB discharges sustain a few seconds with the long live fishbone in the H-mode discharge 80496, the central q profile is flat and $q \sim 1$ inside $\rho < 0.3$. The sustainment of ITB of electron density is accompanied with $m/n = 1/1$ fishbone while it has no fishbone in the phase without ITB at $t = 3.7$ s. Further analysis shows that the $m/n = 1/1$ fishbone signals located at the region of $\rho = 0.3$ which is consistent with central flat q profile and ITB region of electron density. The formation and sustainment of the central flat q profile could be associated with the presence of the fishbone mode. Also, relationship between the formation of ITB and fishbone in EAST high β_N ELMy H-mode discharge is confirmed in discharge 56933 in ref. [1]. This current clamping effect is similar with other hybrid scenarios like in other devices. It suggests that some non-linear coupling exist between the MHD behaviors and the current profiles. The peak of the stored energy during the full shot revealed that the plasma was well constrained.

The $1/1$ mode almost exists during the entire discharge period for improved H mode on EAST, and is a common phenomenon for many similar shots, which is similar to the LLM found on ASDEX-U and MAST [4-6]. The over driven off axis current and fast transport of current from the core area give rise to larger difference between q_{min} and $q=1$ rational surfaces, which makes the internal mode with low m,n number more hard to be driven unstable. The combination of ECRH and LHCD plays an important role in sustaining flat q profile to avoid sawtooth crash. The $1/1$ mode might play important role in shaping current density profile and sustaining the ITB in the high-performance plasma on EAST. The detailed process or mechanism based on internal measurements about how those modes can affect current profile is still missing. In addition those modes may have interactions with background turbulence which need to be further investigated. It is speculated that $1/1$ modes may have interactions with background turbulence and play a role in current relaxation to sustain flat q profile and high-performance plasma with ITB.

. As we all know, ITB formation is always following as the result of suppression of anomalous transport. Figure 8 shows the k spectrum of linear growth rate and frequency of the most unstable modes by TGLF code [36-39] at the typical three time slices in #71326. Growth rate, frequency and poloidal wave number are normalized in form of $\gamma' = \gamma(a/c_s)$, $\omega' = \omega(a/c_s)$ and $k_y = \rho_s k_\theta$, respectively. In which, $c_s = \sqrt{T_e/m_i}$, $\rho_s = c_s/\Omega_s$, $\Omega_s = eB/m_i c$ and length scale a is the circular equivalent minor radius

of the last closed flux surface. As seen in figure8(d), TEM is dominating in the core region and ITG is dominating in the outer region. Thus, growth rate of ITG in the core is lower than TEM and it's much lower than the growth rate of ITG in the outer. Suppression of ITG is strongly relevant with formation of Ti ITB[40].

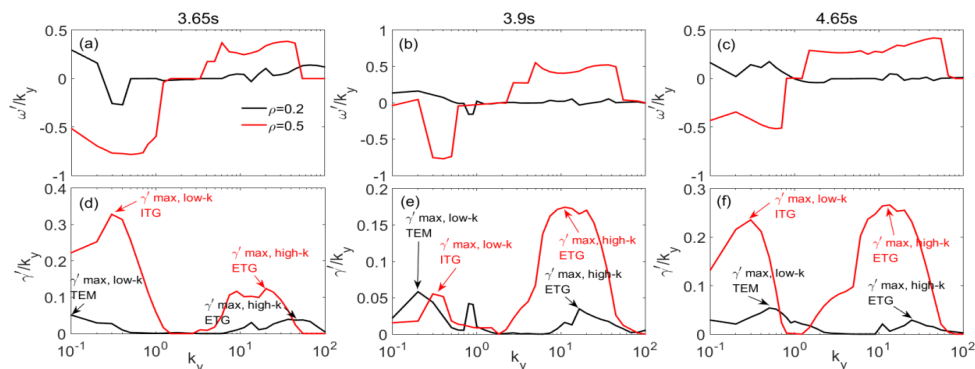


Figure8. Comparison of growth rate(d,e,f) and frequency spectrum(a,b,c) at different position($r=0.2$ is black line, $r=0.5$ is red line) in #71326.

TGLF code is used in gyrokinetic analysis by compute a linearly unstable eigenmodes from the fluid moments equation. The most unstable mode in the selected region could be given. The calculation is based on the reconstructed equilibrium from EFIT code with additional constrained by POINT system. Basic input data of plasma profiles are come from the figure 7. The k spectrum of the linear growth rate and frequency from TGLF is shown in figure 9. Growth rate, frequency and poloidal wave number are normalized in form of $\gamma'=\gamma/(a/c_s)$, $\omega'=\omega/(a/c_s)$ and $k_y=\rho_s k_\theta$, respectively. In which, $c_s = \sqrt{T_e/m_i}$, $\rho_s=c_s/\Omega_s$, $\Omega_s=eB/m_i c$ and length scale a is the circular equivalent minor radius of the last closed flux surface. In these time slices, it is found that the ITG modes dominate in the low- k region where $k_y < 1$ and ETG modes dominate in the high k region($k_y > 1$). The growth rate of ETG is elevated, considering the increasing NBI power while unchanging T_e profiles, ETG induced anomalous electron heating transport raise could be the reason. Unlike the high- k modes, the growth rate of ITG shows a significant decreasing trend in the low- k region. The higher Ti and NBI power do not bring a higher ITG growth rate, frequently burst fishbone shows effect of suppressing the ITG and then leads to the state of sustainment of n_e and Ti ITB.

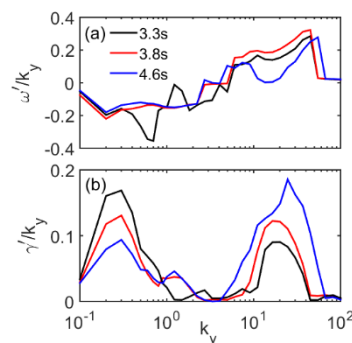


Fig.9 Comparison of growth rate and frequency spectrum with same position(~ 0.2) at different time slices for discharge #71320 from TGLF.

First demonstration of a >100 s time scale long-pulse steady-state scenario with a good plasma performance ($H98(y2) \sim 1.1$, eITB) has been achieved on EAST using the pure radio frequency (RF) power heating and current drive. A typical discharge, with NB injection based on the >100 s long pulse discharge parameter, is shown in Figure 1. Better confinement was obtained with flat central safety factor $q \sim 1$ profile, with a flat boundary is about 0.2 m, and sawtooth-free in plasma discharges, accompanied by a long live mode (LLM) with a few times of current relaxation time. The LLM is localized in the core with the amplitude (10-20 Gauss) directly measured by Faraday-effect based polarimetry, and mode number (1,1) is determined by toroidally and poloidally separate diagnostics. The helical displacement of LLM is estimated to be as large as 2-3 cm, implying helical structure in the core may play an important role in current relaxation to sustain flat q profile

and eITB. The measured local peaking radial magnetic fluctuation of LLM is ~ 90 Gauss, which is at least 10% equilibrium poloidal magnetic field inside $q=1$ surface, suggesting a 3D equilibrium topology.

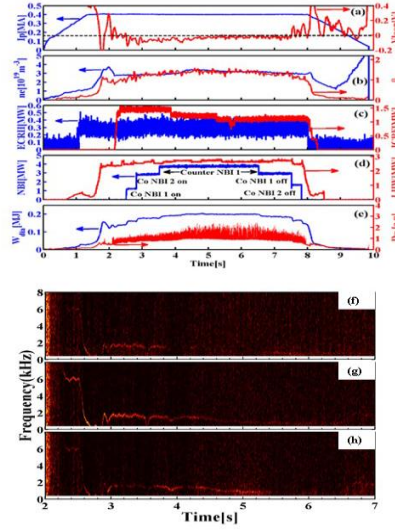


Fig.10 Time history of high beta discharge #70177 with RF & NB (a-e), and Fourier spectra of the Faraday angle signals (f-h).

4. CONCLUSIONS

Substantial progress have been made towards understanding mechanism of ITB in EAST high β experiments. Turbulence induced transport suppression is the key to ITB formation. We focused on ITB formation process on reverse shear and central flat shear separately. Reverse shear is an optimized condition for both electron temperature and ion temperature ITB generation. In this condition, turbulence is suppressed by magnetic shear. Rational minimum value of q in reverse shear could lead to Alfvén cascades, this process is related with emerge of sharp gradient of T_i in the core. The underlying reason is still a mystery and still needs further study. Central flat q profile, with $q_0 \sim 1$, is a sufficient condition for T_e ITB formation with enough electron heating. Electron density ITB can only be observed with MHD behaviors. In EAST high β_N experiment, fishbone always play the important role on ITB formation. It has the same effect on T_i ITB and n_e ITB. Based on different mechanism of MHD, kink mode shows effect on all three channels. In most of these experiments, ITBs are observed which bring the improved confinement. Although the effect of q profiles can't be neglected. MHD behaviors play an important role in many experiments. The fishbone can effectively reduce the power threshold in forming a density ITB in EAST high β_N experiments. The intensity of n_e ITB is not only determined by the heating power, but also decide by the characteristics of fishbone. Simulation of TGLF indicates that higher burst frequency of fishbone can reduce the growth rate of ITG at ITB foot position. ITG dominated particle anomalous transport reduction then contributes to the n_e ITB sustainment. The inference that fishbone leads to better electron density confinement is verified by observation of density gradient increasing with each fishbone burst. While the detailed process of energetic particles redistribution still not been detected directly. Besides, other energetic particles induced mode like Alfvén eigenmode should have the same effect, but there is no experimental result observed on EAST even with several modes reported[41]. With high electron temperature gradient formed, turbulence is driven and it brings a counter direction current perturbation. Excitation of kink mode eliminates the perturbation and reduces turbulence intensity. The feedback loop of the multiscale interaction is the key in high electron temperature long pulse operation. The 1/1 mode might play important role in shaping current density profile and sustaining the ITB in the high-performance plasma on EAST. The detailed process or mechanism based on internal measurements about how those modes can affect current profile is still missing. In addition those modes may have interactions with background turbulence which need to be further investigated. It is speculated that 1/1 modes may have interactions with background turbulence and play a role in current relaxation to sustain flat q profile and high-performance plasma with ITB.

ACKNOWLEDGEMENTS

This work is supported by the National Key R&D Program of China under Grant No. 2017YFE0301205, 2019YFE03040000 and No.2017YFE0301705. This work is also supported in part by Key Program of Research and Development of Hefei Science Center, CAS with contract No. 2019HSC-KPRD001. This work is also partly funded by the National Nature Science Foundation of China with contract No.61627901 and No.6162790105.. This work was partly supported by the Collaborative Research Program of the Research Institute for Applied Mechanics, Kyushu University.

REFERENCES

- [1]. X. Gao. et al 2017 Nucl. Fusion **57** 056021
- [2]. B.N.Wan, et al., Nucl. Fusion **59** 112003(2019)
- [3]. X.Z.Gong, et al., Nucl. Fusion **59** 086030(2019)
- [4] J.Stober et al., Nucl. Fusion **47** 728(2007).
- [5] E. Joffrin et al., Nucl. Fusion **43** 1167(2003).
- [6] I Chapman et al., Nucl. Fusion **50** 045007(2010)
- [7] Hoang G et al 2000 Phys. Rev. Lett., **84** 4593
- [8] Waltz R et al 1997 Phys. Plasmas **4** 2482
- [9] Gormezano C et al 1998 Phys. Rev. Lett., **80** 5544
- [10] Rice J et al 2001 Nucl. Fusion **41** 277
- [11] D.L. Yu et al 2016 Nucl. Fusion **56** 056003
- [12] L.-G. Eriksson et al 2002 Phys. Rev. Lett. **88**.145001
- [13] E. Joffrin et al 2002 Nucl. Fusion **42** 235
- [14] Y. Sakamoto et al 2001 Nucl. Fusion **41** 865
- [15] K.L. Wong et al 2004 Nucl. Fusion **45** 30
- [16] E. Joffrin et al 2003 Nucl. Fusion **43** 1167
- [17] Z.X. Liu et al 2020 Nucl. Fusion **60** 122001
- [18] Li J et al 2013 Nat. Phys. **9** 817
- [19] Wan B et al 2015 Nucl. Fusion **55** 104015
- [20] Liu F et al 2015 Nucl. Fusion **55** 123022
- [21] Hu C et al 2015 Plasma Sci. Technol. **17** 1
- [22] Li Y et al 2014 Rev. Sci. Instrum. **85** 11E428
- [23] Lyu B et al 2014 Rev. Sci. Instrum. Fusion **85** 11E406
- [24] Zang Q. et al 2011 Rev. Sci. Instrum. **82** 063502
- [25] Han X et al 2014 Rev. Sci. Instrum. Fusion **85** 073506
- [26] Liu H.Q. et al 2016 Rev. Sci. Instrum. **87** 11D903
- [27] Zhu X. et al 2015 Plasma Sci. Technol. **17** 9
- [28] Qu H et al 2015 Plasma Sci. Technol. **17** 985
- [29] Qian J et al 2017 Nucl. Fusion **57** 036008
- [30] Tao ZHANG et al 2018 Plasma Sci. Technol. **20** 115101
- [31] Berk H.L. et al 2001 Phys. Rev. Lett. **87** 185002
- [32] Breizman B.N. et al 2003 Phys. Plasmas **10** 3649
- [33] Nazikian R. et al 2003 Phys. Rev. Lett. **91** 125003
- [34] Mingfu WU et al 2020 Plasma Sci. Technol. **22** 025102
- [35] L.Q. Xu, ,Phys. Plasmas **22**,122510(2015).
- [36] Staebler G.M. et al 2005 Phys. Plasmas **12** 102508
- [37] Staebler G.M. and Waltz R.E. 2007 Phys. Plasmas **14** 055909
- [38] Staebler G.M. et al 2013 Phys. Rev. Lett. **110** 055003
- [39] Staebler G.M. 2013 Nucl. Fusion **53** 113017
- [40] E.J. Doyle et al 2002 Nucl. Fusion **42** 333
- [41] Tao ZHANG et al 2018 Plasma Sci. Technol. **20** 115101]